Copyright © 2015 American Scientific Publishers
All rights reserved
Printed in the United States of America

*Journal of Computational and Theoretical Nanoscience*
Vol. 12, 1–6, 2015

# Emergence and Shift of Coulomb Blockade Threshold in Well-Arranged Two-Dimensional Arrays of Nanodots: A Simulation Study

H. Abbasi*, H. Sedghi, and M. Khaje

*Department of Physics, Faculty of Science, University of Urmia, Urmia, Iran*

We present electrical (IV) characteristics of well-arranged multi dot single-electron nanodots—with selected diameters of 1.7, 3 and 6.1 nm-, which composed of several islands up to $30 \times 30$ nanodots. Using SIMON simulator, we investigate emergence of Coulomb blockade in the well-arranged 2D arrays of nanodots. Single electron devices operate based on the Coulomb blockade, therefore we investigate shift in Coulomb blockade threshold voltage upon variation of temperature, size distribution of the nanodots and Length of the arrays. Because of inherent uncertainty in size of nanodots in nano-scale fabrication, we inspect robustness of Coulomb blockade threshold in these array employing Monte Carlo method. We demonstrated that under certain circumstances of size distribution and regularity of nanodot's array, Coulomb blockade emerged in the IV characteristics. Overall, results imply that Coulomb blockade threshold is tolerant to size distribution of nanodots.

**Keywords:** Single Electron Tunneling, Nanodot Array, Coulomb Blockade Threshold, Gaussian Distribution.

RESEARCH ARTICLE

## 1. INTRODUCTION

Nanodot device architecture is one of the ongoing technologies in nano-electronics which has been achieved by continuously shrinking the minimum physical dimensions of the device. Also, recent studies in nanodot architecture such as array architecture assure their important role in nanotechnological applications and make them most suitable for fundamental studies of disordered solids with programmable electronic properties.[1] However, scaling of devices to the nanometer level would face limitations. These limits serve as the motivation to develop new devices and structures at the nanometer scale by conducting their architecture and arrangements.[2–5] One possible novel device is based on the single-electron tunneling and it will be expected to be a key device for future extremely large-scale integrated circuits especially in memory cells because of its low power consumption and small size.

However, single electron devices are very sensitive to background charges, noise energy, defects and size of the islands. Therefore, it is very important to solve problems in order to be able to put single electron circuits into practical use. As a candidate for solving these problems, 2D single electron devices have been proposed. Researches have indicated that multiplexing tunneling junctions are useful for making single electron devices.[6–8] These devices function well in noisy environments, room temperature and also are tolerant against thermal noise, background charges and structure defects with respect to conventional single electron devices. The results obtained from these studies indicated that the functionality of two-dimensional nanodot arrays is expected to be improved when the scale of arrayed nanodots is increased. In the models of multi-dot single-electron devices, the parameters fitting the theory to the experiment are the capacitances and resistances of tunneling junctions.[7] Due to this circumstances, the relationship of the model to the physics of processes in these device structures is lost to a great extent. Solving the models of two-island and multiple-island single-electron chains on the basis of the solution of the Poisson and master equations or using the Monte Carlo method, were suggested previously.[9,10] The multi-dot single-electron devices are promising for the development of a variety of devices due to their smaller size, lower weight, ultra-low power consumption, and higher Coulomb blockade threshold voltage.[8,11–13]

In this paper we present single electron tunneling in well-arranged 2D arrays of nanodots. We investigate IV characteristics of the arrays with controlled size of

*Author to whom correspondence should be addressed.

nanodots for emergence of Coulomb blockade. Our goal of study is to investigate the behavior of Coulomb blockade threshold of these arrays under temperature and size randomization of nanoparticles by Monte Carlo simulation methods. The assumptions and methods used will be described in the following sections.

## 2. ASSUMPTIONS OF THE MODEL AND SIMULATION METHOD

We selected nanodots with diameters of 1.7, 3 and 6.1 nm according to fabricated nanodots. The diameter of these nanodots show Gaussian distribution with narrow full widths at half maximum (FWHMs).[14] The extracted data from experimental results are shown in Table I. We assumed well-arranged $10\times 10$, $20\times 20$, and $30\times 30$ arrays of nanodots with Gaussian distribution in diameter. Schematic diagram of the considered configurations are shown in Figure 1.

The arrays were biased by a source–drain voltage $V_{\mathrm{ds}}$ and was set from 0 to 20 V. Figure 2 shows equivalent circuits for assumed configuration of nanodots in Figure 1. If the widths of the gaps between adjacent nanodots be small, each less than 10 nm, then an applied potential difference greater than Coulomb blockade threshold voltage between the electrodes can transfer electrons on to and off the dots by quantum mechanical tunneling.[15] The gaps then form tunnel barriers, with an associated energy barrier. In such a systems single electron tunneling occurs. The mean widths of tunneling gaps are provided in Table I.

Using SIMON2.0 single-electron device simulator, we investigated $I_{\mathrm{ds}}$–$V_{\mathrm{ds}}$ characteristics of equivalent circuits consisting nanodots and tunneling junctions. The results from simulations of $10\times 10$, $20\times 20$ and $30\times 30$ arrays are provided in results and discussion section. The SIMON 2.0 is a single-electron device and circuit simulator which employs Orthodox theory and Monte-Carlo methods in order to simulate the propagation of electrons in a wide variety of single-electron circuits.[16] Orthodox theory is a semi-classical approach, which assumes that

(i) the energy spectrum of the conductive islands may be considered continuous
(ii) the tunneling time is negligible compared to the time between tunneling events, and
(iii) coherent tunneling events are ignored.[17]

The essential parameters in the multi-dot single-electron devices are resistance and capacitance of tunneling junctions. We assume that the resistance of tunneling junctions can be described by:[18,19]

$$R \propto e^{\beta L} e^{E_{\mathrm{C}}/kT} \tag{1}$$

Where $L$ is the size of the tunneling gap. Here, the activation energy $E_{\mathrm{C}}$ is the Coulomb charging energy and $\beta$ is a system dependent tunneling constant given by $\beta = \sqrt{8mU_0/\hbar^2}$,[18] with $m$ as effective mass of an electron. For avoiding several simultaneous tunneling, minimum tunnel resistance of all the tunnel barriers must be much higher than quantum unit of resistance $R_Q$ ($R \gg R_Q = h/e^2 \sim 26.5\ \mathrm{K\Omega}$), where $e$ is the elementary charge of electron and $h$ is Plank constant.[20,21]

We used an analytical method employing image charges for the calculation of junction capacitances $C_{ij}$ between neighboring islands:[22,23]

$$C_{12} = \frac{4\pi\epsilon_0 ab}{c}\sinh(U)\sum_{n=1}^{\infty}[\sinh(nU)]^{-1} \tag{2}$$

Where $a$ and $b$ are the radii of nanodots and dimensionless parameter $U$ is related to $a$, $b$ and $c$ by $\cosh(U) = (c^2 - a^2 - b^2)/(2ab)$. Here, $c$ is the center-center distance between adjacent nanodots.

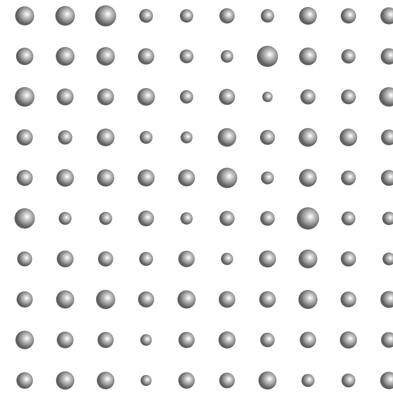

**Fig. 1.** Schematic diagram of well arranged 2D array of nanodots.

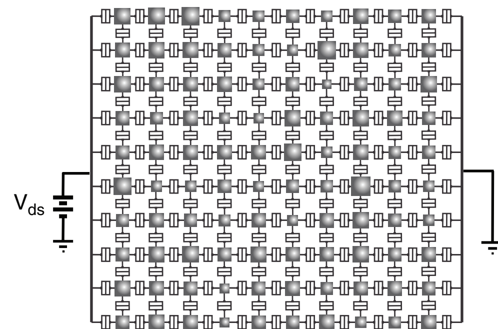


**Fig. 2.** Schematic circuit diagram of well-arranged 2D arrays of nanodots.

**Table I.** A summery of parameters used in simulations.

| | | | |
|---|---|---|---|
| Mean diameter of nanoparticles | 1.7 | 3 nm | 6.1 nm |
| Full width at half maximum (nm) | 0.65 | 0.66 | 0.7 |
| Mean tunneling gap between nanodots (nm) | 1.9 | 2.25 | 3.4 |

According to the literature, Coulomb blockade threshold voltage for 1D array of nano-islands is related to:[17,24]

$$V_{\mathrm{th}} \propto \frac{N}{C_{\Sigma}} \tag{3}$$

Where $N$ is the number of junctions and $C_{\Sigma}$ is total capacitance of the chain. This is achieved under the above conditions for tunnel resistance. The linear relationship shown above between the threshold voltage ($V_{\mathrm{th}}$) and the number of junctions ($N$) has also been observed in 2-dimensional systems.[25,26]

Furthermore, the temperature of 10, 110, and 300 K were selected for simulations. After setting some parameters like temperature, mode of simulation, resistance and capacitance of tunneling junctions, We inspected IV characteristics.

## 3. DISCUSSION AND RESULTS

Figure 3 shows the $I_{\mathrm{ds}}$–$V_{\mathrm{ds}}$ for $10\times 10$, $20\times 20$, and $30\times 30$ arrays of nanodots at 110 K. Also shown in this figure are the size distribution of nanodots. Coulomb blockade are clearly observed. At bias voltages more than threshold voltage the dc curve gradually approaches to offset linear asymptotes. The scales are in good agreement with other results in the literature.[8] Extrapolation of the linear regions result in a $V_{\mathrm{th}}$ given in Table II for arrays with mean diameter of 1.7, 3 and 6.1 nm which represent the basic conceptual principle of threshold voltage.[27] we remark that the current suppression region for arrays decreases with increasing mean diameter of nanodots. In the literature, Coulomb blockade threshold for a 1D array of nano-islands is inversely related to the capacitance, therefore, in 2D arrays the decreasing in current suppression region is probably due to the increase in the total capacitance of the array.

By increasing the length of the arrays, Coulomb blockade threshold voltage increases, as can be seen in Figure 3. Since essential parameters in the single electron tunneling are tunneling capacitance and resistance, thus this increase is probably due to decrease in the total capacitance of the arrays. We found the increase in the Coulomb blockade threshold voltage with length of the array is linear which is in agreement with results in the literatures (Fig. 4). We remark that, it's the length of the array that determines the value of Coulomb blockade threshold voltage.

Fabricated nanodots have inherent randomization in their size. We randomized diameter of nanodots according to the the Gaussian distribution shown in Figure 3. We carried out 100 simulations in which diameter of any individual nanodot in the arrays were changed randomly in each simulation. IV characteristics were plotted each time and coulomb blockade threshold was observed for each array. The results of these simulations for $10\times 10$ arrays are shown in Figure 5. As it can be seen from Figure 5,

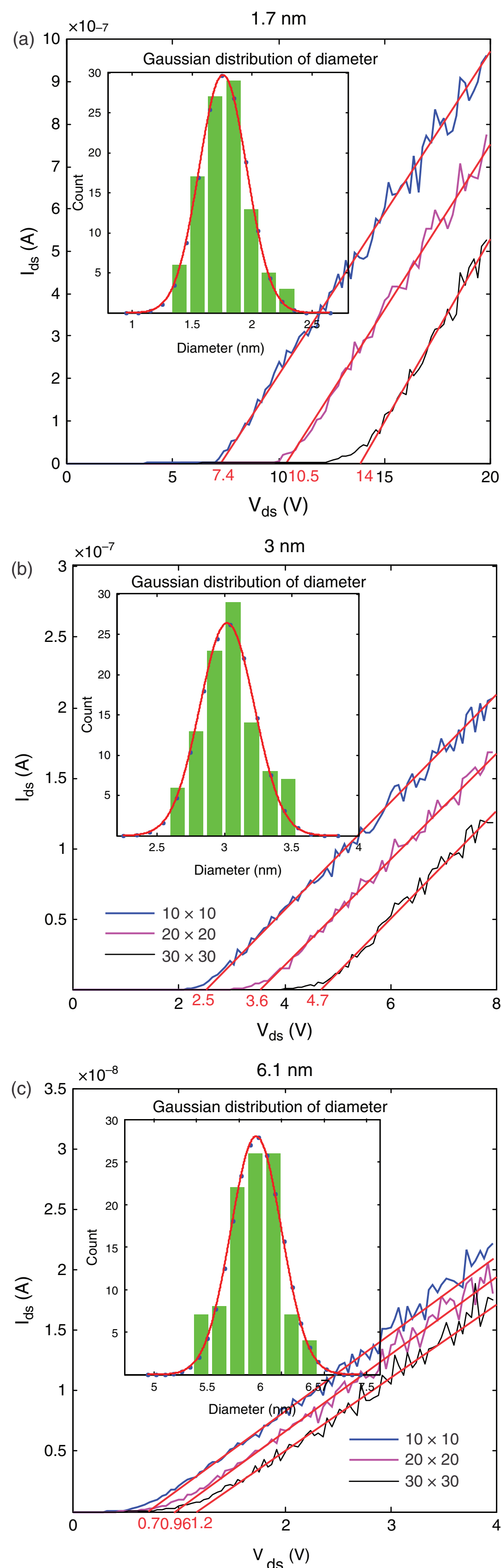


**Fig. 3.** $I_{\mathrm{ds}}$–$V_{\mathrm{ds}}$ characteristics of arrays, respectively, for (a) 1.7, (b) 3, and (c) 6.1 nm nanodots simulated at $T = 110$ K.

RESEARCH ARTICLE

**Table II.** $V_{th}$ calculated from extrapolation of linear regions to zero.

| Mean diameter of nanoparticles | 1.7 | 3 nm | 6.1 nm |
|---|---|---|---|
| $V_{th}$ for $10 \times 10$ arrays of nanodots (V) | 7.4 | 2.5 | 0.7 |
| $V_{th}$ for $20 \times 20$ arrays of nanodots (V) | 10.5 | 3.6 | 0.96 |
| $V_{th}$ for $30 \times 30$ arrays of nanodots (V) | 14 | 4.7 | 1.2 |

IV characteristics overlap and Coulomb blockade threshold do not changes. These results show that IV characteristics of these arrays are not dependent on the diameter of individual nanodot. In fact, Whilst size of nanodots obey Gaussian distribution, the size of individual nanodot is not important.

We observed the $V_{th}$ of the arrays at selected temperatures of 10, 110, and 300 K. The effect of temperature on the $V_{th}$ of nanodots are shown in Figure 6. By increasing temperature, $V_{th}$ decreases which means that $k_B T$ becomes comparable to the charging energy and thermal fluctuations suppress single electron effects. With decreasing the diameter of nanodots, Coulomb blockade threshold become tolerant against increasing temperature since charging energy becomes greater than $k_B T$.

We also investigated the IV characteristics of the arrays when FWHM in Gaussian distribution of the arrays broadens. Figure 7 shows IV characteristics for arrays with different Gaussian distribution considered for diameter of nanodots. As it can be seen from Figure 7 Coulomb blockade threshold do not changes by increasing the FWHM of the nanodots. The possible reason for not changing the Coulomb blockade threshold is that the paths consisting nanodots with mean diameter is dominant in the array.

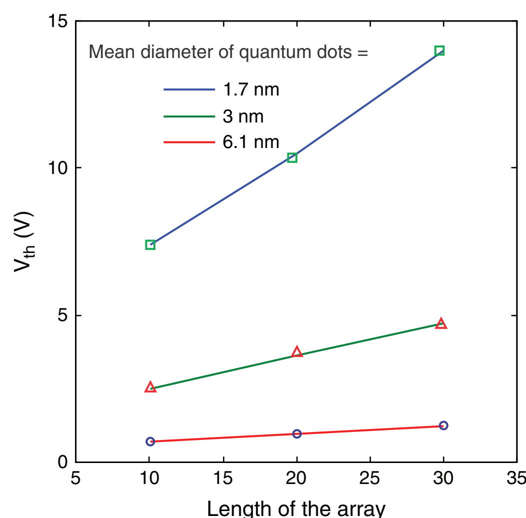


**Fig. 4.** Variation of $V_{th}$ versus length of the array.

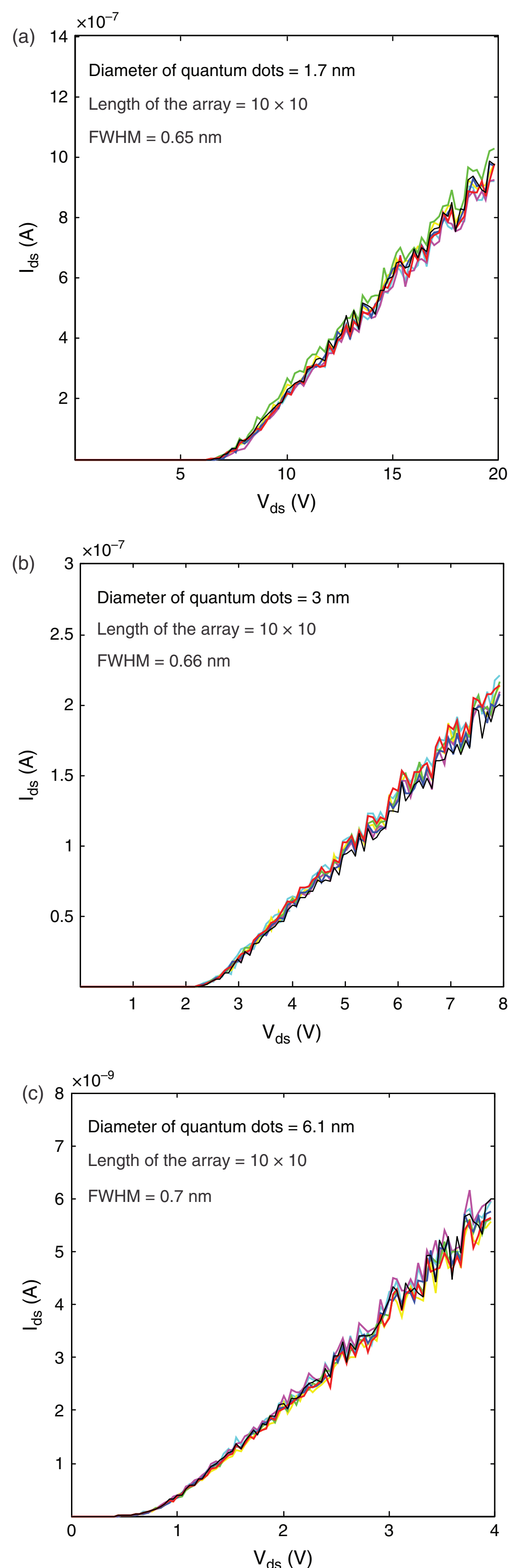


**Fig. 5.** Monte Carlo study on the $V_{th}$ by size randomization.

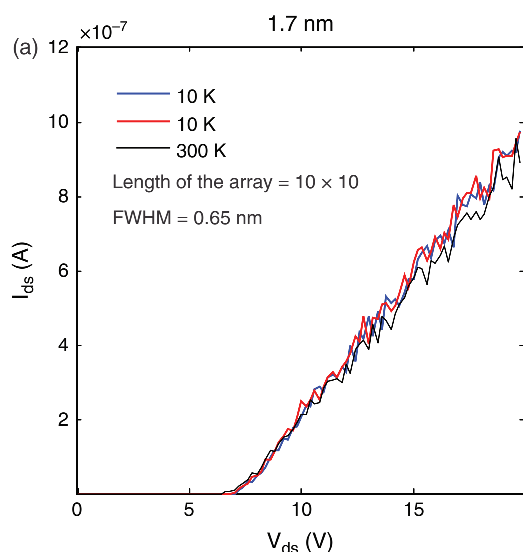


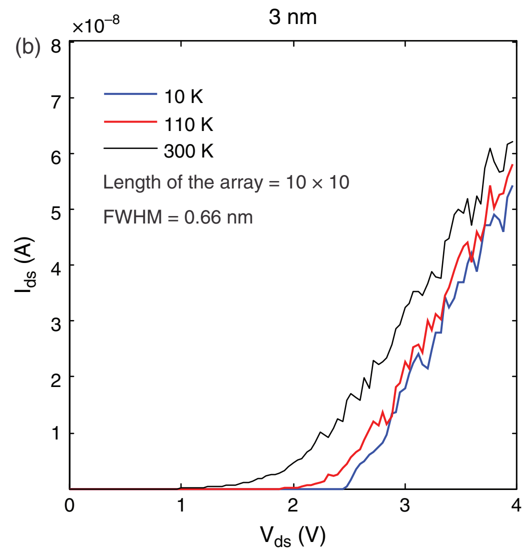


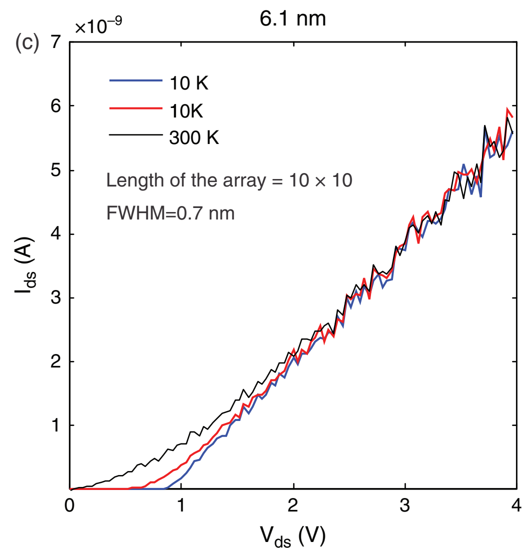


**Fig. 6.** Variation of $V_{th}$ versus temperature, respectively, for (a) 1.7, (b) 3, and (c) 6.1 nm nanodots.

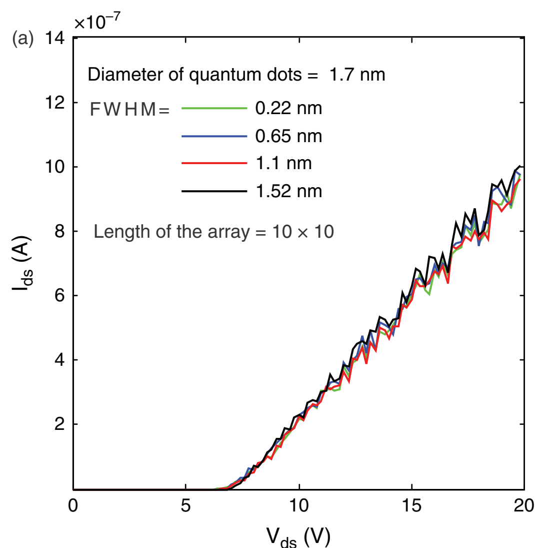


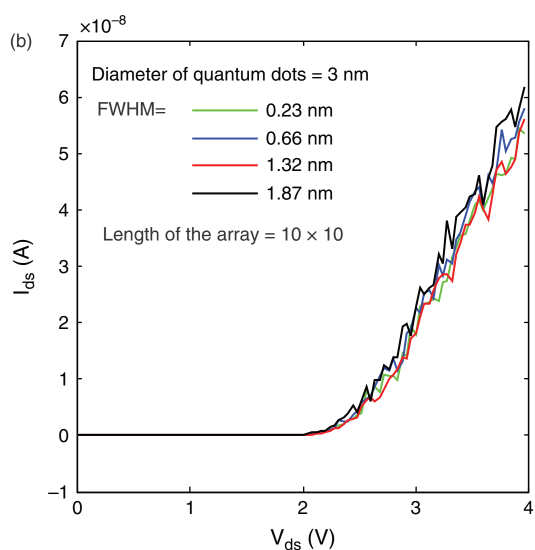


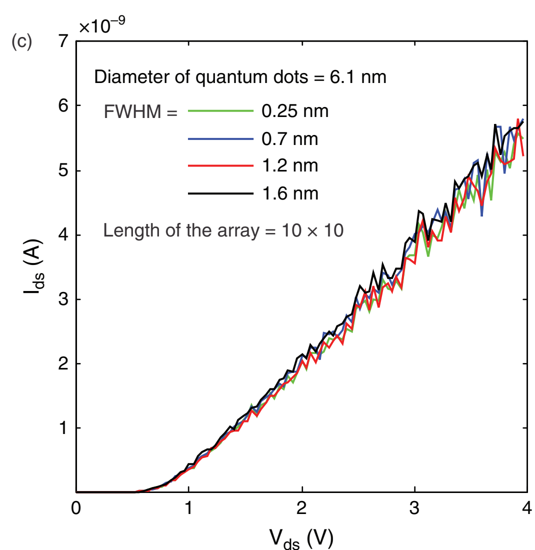


**Fig. 7.** Effect of Gaussian distribution on the Coulomb blockade threshold voltage.

RESEARCH ARTICLE

## 4. CONCLUSIONS

Possibility of single electron tunneling in well-arranged 2D arrays of nanodots with gaussian distribution in diameter, were confirmed by simulation methods. Coulomb blockade threshold in the IV characteristics of arrays with selected size of nanodots arranged in regular lattice was observed. Coulomb blockade threshold voltage had a linear relation versus Length of the array which is in agreement with previous works. Also results depicts that with increasing mean diameter of the nanodots in the arrays, $V_{th}$ decreases which according to relation (3) may be related to the increasing total capacitance of the arrays. Arrays of nanodots with sizes obeying Gaussian distribution are tolerant to the size distribution of nanodots and with increasing the FWHM of the Gaussian distribution $V_{th}$ not changes since dominant path are consisted from nanodots with mean diameter of nanodots.

## References


1. K. K. Ostrikov, U. Cvelbar, and A. B. Murphy, *Journal of Physics D: Applied Physics* 44, 174001 (**2011**), http://stacks.iop.org/0022-3727/44/i=17/a=174001.
2. R. Sachser, F. Porrati, and M. Huth, *Phys. Rev. B* 80, 195416 (**2009**).
3. M. Jo, T. Kaizawa, M. Arita, A. Fujiwara, K. Yamazaki, Y. Ono, H. Inokawa, Y. Takahashi, and J.-B. Choi, Silicon nanodot-array device with multiple gates, Materials Science in Semiconductor Processing 11, 175 (**2008**); *e-MRS 2008 Spring Conference Symposium J: Beyond Silicon Technology: Materials and Devices for Post-Si {CMOS}*, doi:http://dx.doi.org/10.1016/j.mssp.2008.12.001, URL http://www.sciencedirect.com/science/article/pii/S1369800108000929.
4. Q. Wang, Y. Chen, S. Long, J. Niu, C. Wang, R. Jia, B. Chen, M. Liu, and T. Ye, *Microelectronic Engineering* 84, 1647 (**2007**), *Proceedings of the 32nd International Conference on Micro- and Nano-Engineering*, doi:http://dx.doi.org/10.1016/j.mee.2007.01.261, URL http://www.sciencedirect.com/science/article/pii/S0167931707002365.
5. F. Porrati, R. Sachser, M. Strauss, I. Andrusenko, T. Gorelik, U. Kolb, L. Bayarjargal, B. Winkler, and M. Huth, *Nanotechnology* 21, 375302 (**2010**), URL http://stacks.iop.org/0957-4484/21/i=37/a=375302.
6. M. A. Rafiq, K. Masubuchi, Z. A. K. Durrani, A. Colli, H. Mizuta, W. I. Milne, and S. Oda, *Jpn. J. Appl. Phys.* 51, 025202 (**2012**).
7. A. Boubaker, M. Troudi, N. Sghaier, A. Souifi, N. Baboux, and A. Kalboussi, *Microelectronics Journal* 40, 543 (**2009**); *Workshop of Recent Advances on Low Dimensional Structures and Devices (WRA-LDSD)*, doi:http://dx.doi.org/10.1016/j.mejo.2008.06.089.
8. H. Mehrara, A. Erfanian, M. Khaje, M. Zahedinejad, and F. Rezvani, *Superlattices Microstruct.* 53, 1 (**2013**),
9. I. Abramov, S. Ignatenko, and E. Novik, *Semiconductors* 36, 1192 (**2002**).
10. I. Abramov, S. Ignatenko, and E. Novik, *Semiconductors* 37, 564 (**2003**).
11. X. Zhang, Y. Chi, J. Fang, H. Zhong, S. Chang, L. Fang, and S. Qin, *Phys. Lett. A* 374, 4880 (**2010**).
12. P. Karre, M. Acharya, W. Knudsen, and P. Bergstrom, *IEEE Sens. J.* 8, 797 (**2008**).
13. H. Fujino and T. Oya, *Jpn. J. Appl. Phys.* 53, 06JE02 (**2014**).
14. B. Ingham, M. F. Toney, S. C. Hendy, T. Cox, D. D. Fong, J. A. Eastman, P. H. Fuoss, K. J. Stevens, A. Lassesson, S. A. Brown, and M. P. Ryan, *Phys. Rev. B* 78, 245408 (**2008**).
15. D. Averin and K. Likharev, *J. Low Temp. Phys.* 62, 345 (**1986**).
16. C. Wasshuber and H. Kosina, *Superlattices Microstruct.* 21, 37 (**1997**).
17. K. Likharev, *Proceedings of the IEEE* 87, 606 (**1999**).
18. B. Barwiski, *Thin Solid Films* 148, 233 (**1987**).
19. J. van Lith, A. Lassesson, S. A. Brown, M. Schulze, J. G. Partridge, and A. Ayesh, *Appl. Phys. Lett.* 91 (**2007**), doi:http://dx.doi.org/10.1063/1.2802730.
20. D. Averin and A. Odintsov, *Phys. Lett. A* 140, 251 (**1989**). URL http://www.sciencedirect.com/science/article/pii/0375960189909341.
21. L. J. Geerligs, D. V. Averin, and J. E. Mooij, *Phys. Rev. Lett.* 65, 3037 (**1990**).
22. E. Pisler and T. Adhikari, *Phys. Scr.* 2, 81 (**1970**).
23. J. Lekner, *J. Electrostat.* 69, 11 (**2011**).
24. M. A. Savaikar, D. Banyai, P. L. Bergstrom, and J. A. Jaszczak, *J. Appl. Phys.* 114 (**2013**), doi:http://dx.doi.org/10.1063/1.4821224, URL http://scitation.aip.org/content/aip/journal/jap/114/11/10.1063/1.4821224.
25. R. Parthasarathy, X.-M. Lin, K. Elteto, T. F. Rosenbaum, and H. M. Jaeger, *Phys. Rev. Lett.* 92, 076801 (**2004**). URL http://link.aps.org/doi/10.1103/PhysRevLett.92.076801.
26. R. Parthasarathy, X.-M. Lin, and H. M. Jaeger, *Phys. Rev. Lett.* 87, 186807 (**2001**). URL http://link.aps.org/doi/10.1103/PhysRevLett.87.186807.
27. A. Ortiz-Conde, F. G. Snchez, J. Liou, A. Cerdeira, M. Estrada, and Y. Yue, *Microelectronics Reliability* 42, 583 (**2002**).


Received: 5 March 2015. Accepted: 24 March 2015.